# Concurrent Estimation of Finger Flexion and Extension Forces using Motoneuron Discharge Information

Yang Zheng and Xiaogang Hu

Abstract— Objective: A reliable neural-machine interface offers the possibility of controlling advanced robotic hands with high dexterity. The objective of this study was to develop a decoding method to estimate flexion and extension forces of individual fingers concurrently. Methods: First, motor units (MUs) firing information were identified through surface electromyogram (EMG) decomposition, and the MUs were further categorized into different pools for the flexion and extension of individual fingers via a refinement procedure. MU firing rate at the populational level was calculated, and the individual finger forces were then estimated via a bivariate linear regression model (neural-drive method). Conventional EMG amplitude-based method was used as a comparison. Results: Our results showed that the neural-drive method had a significantly better performance (lower estimation error and higher correlation) compared with the conventional method. Conclusion: Our approach provides a reliable neural decoding method for dexterous finger movements. Significance: Further exploration of our method can potentially provide a robust neural-machine interface for intuitive control of robotic hands.

Index Terms— Finger force estimation, Flexion and extension, Isometric contractions, Neural-machine interface, Neural-decoding

# I. INTRODUCTION

A reliable neural-machine interface allows intuitive interaction with assistive devices such as prostheses and exoskeletons [1] or remote control of devices [2]. In the past few decades, substantial scientific and technological efforts have been made to develop central and peripheral neural interfaces between humans and machines [3, 4]. Among these neural signals, sEMG has been widely used in neural-machine interface [5, 6], largely because sEMG can be obtained non-invasively and can yield segregated neural activities of individual muscles. As a result, sEMG-based interface can be used to control robotic devices with multiple degrees of freedom. For example, with pattern recognition of sEMG signals of both extrinsic and intrinsic muscles, up to 19 hand gestures can be identified with an accuracy of 96% [7]. However, pattern recognition can only specify a discrete

Yang Zheng (email: yang 1127@email.unc.edu) and Xiaogang Hu (email: xiaogang@unc.edu) are with the Joint Department of Biomedical Engineering at University of North Carolina-Chapel Hill and NC State University (correspondence e-mail: xiaogang@unc.edu)

number of states [8]. In order to control individual degrees of freedom in a continuous manner, proportional control was needed to improve intuitive control. Specifically, EMG global features, such as the amplitude, are extracted as the control input signals. However, the control performance can degrade over time, since the EMG amplitude can be affected substantially by factors such as motion artifact, background noise, and muscle fatigue. In addition, the cancellation and summation of superimposed motor unit action potentials (MUAPs) from different motor units (MUs) can lead to complex relation between the level of muscle contraction and EMG amplitude.

Instead of using global EMG features, MU firing activity has been used as an alternative neural interface. Specifically, populational MU firing frequency reflects the neural drive input to the motoneuron pool and can be used to estimate the muscle activation level [9]. The decoded motoneuron activity has been used to predict joint kinematics of wrist [10, 11] or fingers [12, 13]. In addition, it has also been demonstrated that the MU firing information is more robust to estimate the isometric finger extension force for both intact [14, 15] and stroke subjects [16], compared with the conventional EMG method. On average, the error between the measured and estimated forces decreases by 16.03% and 22.45% for intact and stroke subjects, respectively, using the MU firing information. However, these studies only focused on finger extension. To enable dexterous finger movement, finger force estimation needs to be performed when both finger flexion and extension are involved. Despite the success of estimating isometric finger extension force, it remains a big challenge to estimate the finger flexion and extension force concurrently in a dexterous manner. First, the flexor digitorum superficialis (FDS) muscle is located relatively far away from the skin, making it difficult to reliably extract MU firing activities specific to individual fingers. Second, finger enslavement from co-activation of flexor or extensor muscle compartments poses additional challenge to estimate individual finger forces. Lastly, co-activation of agonist-antagonists can occur during fine motor control [17, 18]. This means that the net extension or flexion force of a specific finger is not determined by the activation of just extensor or flexor muscles, but a combination of both muscles. However, as far as we know, no previous studies have investigated the net effect of neural drive to

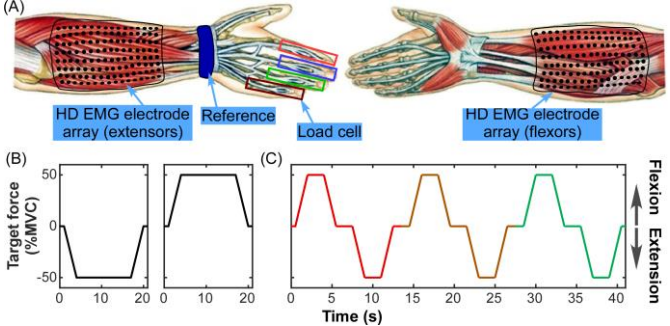


Fig. 1. Monopolar EMG signals were recorded from the finger extensor and flexor, respectively, with two 8×16 electrode arrays, and the flexion/extension forces of the index, middle, ring, and pinky fingers were recorded (A). The trapezoidal force target from the single-finger extension and flexion trial (B) and the multi-finger trial (C). The force target of the multi-finger trial was shown with different colors to represent the three fingers, i.e. index (red), middle (brown), and ring-pinky (green) as the target finger, respectively.

agonist-antagonist muscles, in terms of net force output.

To address these issues, we developed a force estimation method based on MU firing activities, in order to estimate the individual fingertip forces concurrently during dexterous finger flexion and extension. Specifically, High-density EMG (HD-EMG) signals were recorded from the finger flexors and extensors. The MU firing events were extracted through a source separation algorithm, and were further classified into different pools associated with the flexion and extension of individual fingers. Then, the MU firing rate in each pool was calculated to estimate the neural-drive (neural command), and a regression model was then used to estimate individual finger forces based on the finger-specific neural-drive. conventional EMG amplitude-based method was performed as a comparison. The results showed that the force estimation performance of the neural-drive method was significantly better (a higher correlation and a smaller estimation error between the estimated force and the measured force) than that of the conventional method. The neural-drive method also showed a larger estimation error in finger flexion than extension, which was partly due to a smaller number of identifiable MUs from the flexor compared with the extensor. Overall, our method can potentially provide a robust neural-machine interface for intuitive control of advanced robotic hands.

# II. METHODS

# A. Experiment

# 1) Subjects

Seven neurologically intact participants (age: 21–35) were recruited in the study. All subjects gave informed consent with protocols approved by the Institutional Review Board of the University of North Carolina at Chapel Hill.

## 2) Data recording

Two 8×16 electrode arrays with a 3 mm single-electrode diameter and a 10 mm inter-electrode distance covered the anterior and posterior sides of the forearm to record EMG signals from the finger flexor (FDS) and extensor (extensor digitorum communis (EDC)), respectively (Figure 1 A). The

placement of the electrode was determined by palpating the finger flexor or extensor when the subjects flexed or extended fingers. The EMG-USB2+ (OT Bioelettronica) system was used to amplify and sample the monopolar EMG signals with a gain of 1000, a pass band of 10-900 Hz and a sampling rate of 2048 Hz. The reference was placed at the wrist.

The index, middle, ring, and pinky fingers were individually secured to four miniature load cells (SM-200N, Interface), to measure the flexion and extension forces of individual fingers at 1000 Hz (Figure 1 A). The forearm was supported at the neutral position with the wrist fixed by two stiff foam pads, in order to minimize the force transmission from the wrist to the load cells. Before each trial, the offsets of individual load cells were removed such that a positive force reading represented flexion and a negative reading represented extension.

## 3) Experiment procedure

The maximum voluntary contraction (MVC) force was first measured for the flexion and extension of individual fingers. During the main experiment, the subject was requested to follow a predefined force target that had a repeated trapezoidal pattern with a maximum force of 50% MVC of each finger (Figure 1 B and C). The 50% MVC was selected to avoid muscle fatigue at higher force levels, and was sufficient to induce co-activations between muscle compartments and between agonist-antagonist musles. Due to high enslavement between ring and pinky fingers [19], the subjects were requested to extend or flex the two fingers simultaneously all the time, and the two fingers were considered as one finger (ring-pinky finger in the subsequent text) during the main experiment and data processing. The MVC of the ring-pinky finger was the summation of the MVC of the ring and pinky fingers. The force measurements from the ring and pinky fingers were always summed up before displaying to the subjects on the monitor.

Subjects performed two different types of trials. The first type involved the flexion or extension of a single finger (single-finger trial) and the force target contained a single trapezoid (Figure 1 B). During the single-finger trials, the subjects were requested to avoid co-contractions of other fingers. Four single-finger trials were performed for the flexion and extension, respectively, resulting in eight single-finger trials for each finger. The second type involved at least two fingers flexing and extending sequentially (multi-finger trial). The force target of a multi-finger trial with finger (index, middle, and ring-pinky) flexion and extension in sequence is illustrated in Figure 1 C. Within a given period of individual trapezoidal force target of the multi-finger trials, one finger (target finger) was requested to flex or extend to maintain the targeted force, while the requirement of the other two fingers (non-target finger) was not specified (i.e., co-activation was allowed). The order of the target fingers was randomized across the multi-finger trials. Each subject performed a total of 16 multi-finger trials.

## B. Data processing

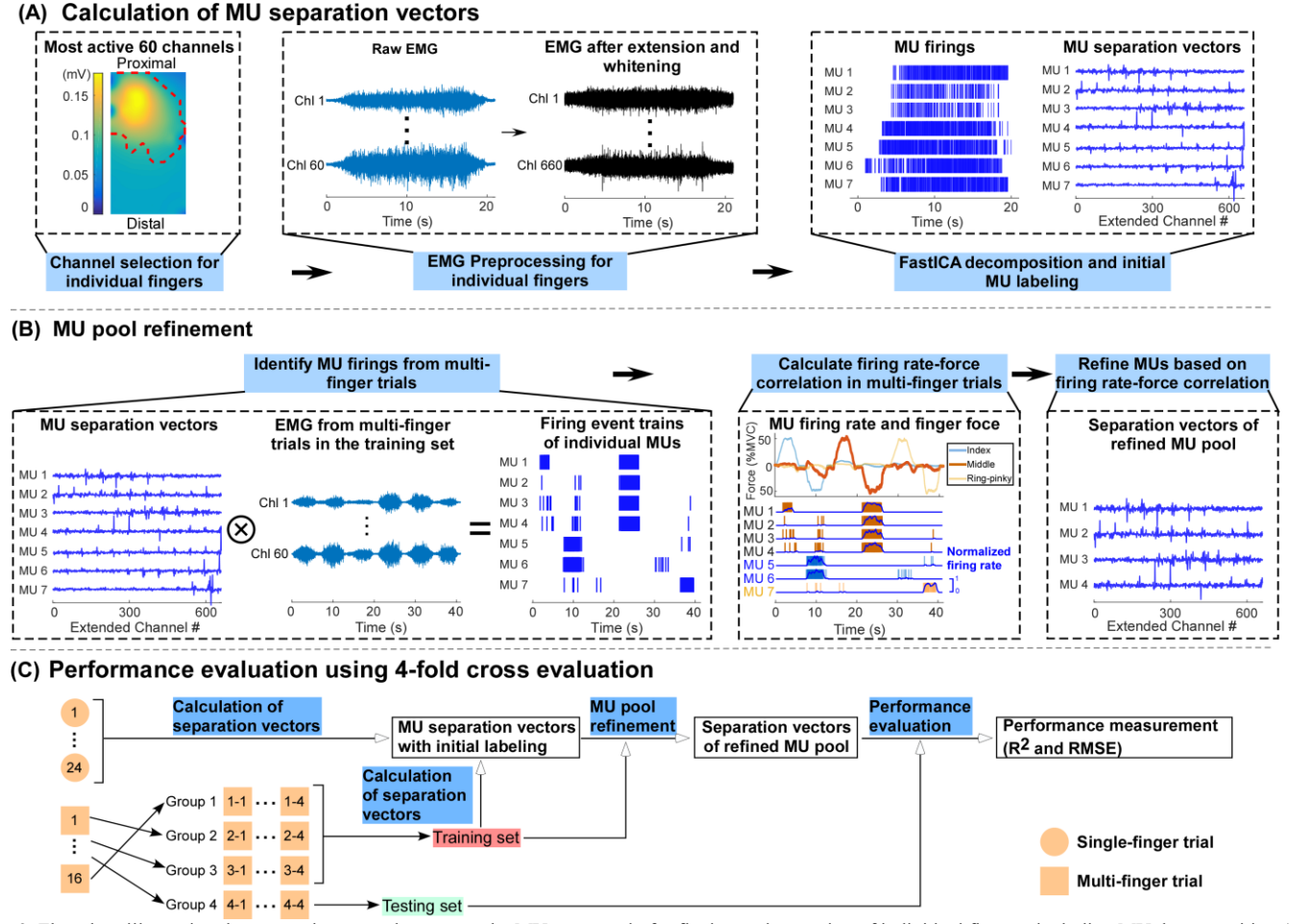


Fig. 2. Flowchart illustrating the processing steps that extract the MUs separately for flexion and extension of individual fingers, including MU decomposition (A) and MU pool refinement (B). The extension of the middle finger was used as an example.  $\otimes$ : apply the separation vectors to EMG signals after extension and whitening. The performance evaluation procedure of one of the 4-fold cross-evaluations (C). After the 4-fold evaluation, each group was used as the testing set once.

A high pass filter (Butterworth zero-phase shift with an order of 4 and a cutoff frequency of 10 Hz) was used to filter all the EMG signals, and motion artifacts were removed using a previously developed method [20].

1) Force estimation using the MU discharge information Calculation of MU separation vector (Figure 2 A). In order to reduce the computational load, only 60 out of the 128 channels were used to perform EMG decomposition for the flexion or extension of each finger. Specifically, the EMG amplitude (root mean square, RMS) was calculated for all 128 channels from the corresponding flexor or extensor muscles using the single-finger trials, and then averaged across all the single-finger trials. The top 60 channels with the maximum amplitude were used to extract MU separation vectors. The selection of 60 was based on our preliminary test to balance computational time and the accuracy of MU information. Figure 3 B and C illustrate the EMG amplitude (RMS) when individual fingers flexed or extended in a multi-finger trial (Figure 3 A), and the red curves encircled the 60 channels used for EMG decomposition. The selected channels covered the most active area under different conditions.

The MU discharge information was obtained through the EMG decomposition procedure, using the Fast Independent Component Analysis (FastICA) algorithm [21-23]. The detailed decomposition steps are in the Supplementary Material.

Briefly, EMG signals were first preprocessed through a signal extension (extension factor of 9) and whitening procedure. The extension procedure added 9 delayed versions of each channel, resulting in 600 channels in total after extension. Through a fixed-point iteration procedure, the FastICA method can obtain the separation vectors and the source signals of individual MUs from a given segment of preprocessed HD-EMG signals. The source signal can be further converted into discharge event train via a Kmeans++ cluster algorithm [24, 25] for binary classification.

Both the single-finger trials and the multi-finger trials were used to obtain the MU separation vectors. When the single-finger trials were used, the 60 channels of the target finger of a trial were used, and the decomposed MUs were initially labeled with a specific finger (index, middle, and ring-pinky) and a motion type (flexion or extension). When decomposing the multi-finger trials, the MU separation vectors were obtained for the flexion and extension of individual fingers separately. The co-contraction in the multi-finger trials can help to identify some MUs recruited at low contraction levels for individual fingers, which can improve the force estimation performance when the contraction force level was low. To this end, six MU pools were obtained corresponding to the flexion and extension of three fingers, respectively. The classification of MUs into individual pools was based on the

tested finger and the EMG channels used to perform EMG decomposition. This was a preliminary labeling procedure, because the EMG channels used for different fingers had substantial overlap, and co-contractions could occur in the single-finger trials. Therefore, a refinement procedure was needed to further refine the MU pools for the flexion and extension of individual fingers.

MU pool refinement (Figure 2 B). The MU pools were refined using the multi-finger trials. The rationale was that the MU firing rate associated with a given finger should be modulated by that given finger force, and should therefore have a high correlation with the force of the given finger. Accordingly, the MU separation vectors obtained earlier were applied to the EMG data of the multi-finger trials to calculate the MU discharge events. The event trains were then processed using a 1-second average window with a 0.1-second moving step (in subsequent text, the average windows were all the same unless otherwise noted), resulting in the time courses of firing rate for individual MUs. Meanwhile, the force data of three fingers were also smoothed using the average window. For a given MU from the pool, a regression analysis was performed between the firing rate and the smoothed force of the three fingers. Before the regression analysis, if the MU pool was associated with finger flexion, the extension force data were set to zero, and vice versa. The coefficients of determination (r-squared, R<sup>2</sup>) values were obtained for each finger. If the R<sup>2</sup> value of the specific finger was larger than that of the other two fingers, the MU was kept. Otherwise, it was removed from the MU pool. After the regression analysis and R<sup>2</sup> comparison were performed for all the MUs, the MU pool was refined.

Performance of force estimation. During the force estimation procedure, the separation vectors were directly applied to the new EMG data. The discharge events of MUs with known finger labels were obtained, which has been used in our previous study to obtain the MU discharge information in real-time [14]. In order to avoid in-sample optimization, the multi-finger trials were divided into training and testing sets, with the training set for MU separation vector calculation and MU pool refinement and the testing set for force estimation. Specifically, a four-fold cross-evaluation was performed. The multi-finger trials were divided into 4 equal groups. For each fold, one group was selected as the testing set and the other 3 groups constituted the training set. The final force estimation performance was obtained by averaging across all folds of evaluations (Figure 2C).

The force estimation was performed using the multi-finger trials in the testing set. The firing event trains of individual MUs from the refined pool were first obtained. Then, the populational MU firing rate was calculated using the average window for each refined pool. Since no previous studies have explored the relation between the net force and the neural drive signal of the flexors and the extensors, a simple linear relation was hypothesized to exist between the three variables. Therefore, a bivariate linear regression analysis was performed between the smoothed force data and the populational firing rate of MUs specific to the flexors and extensors for individual fingers.

$$F_i = aD_{i,flx} + bD_{i,ext} \tag{1}$$

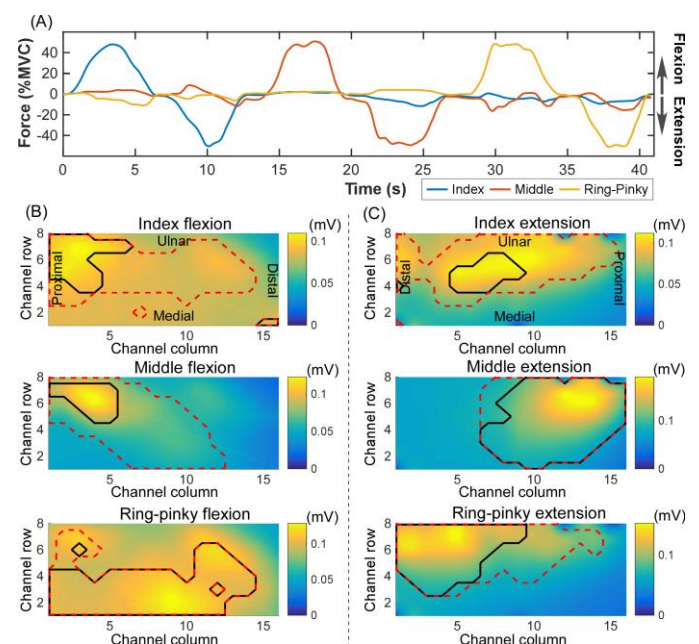


Fig. 3. The force data from a representative multi-finger trial (A). The EMG amplitude (root mean square) distribution when individual fingers flexed (B) and extended (C). The EMG segments used to calculate the EMG amplitude corresponded to the plateau period of the force target shown in Figure 1 B. The red dashed lines encircled the 60 channels used to perform EMG decomposition for the flexion and extension of individual fingers. The back solid line encircled the channels used to estimate the EMG amplitude for the flexion and extension of individual finger in the EMG-amp method.

where  $F_i$  is the force of the *i*th finger (i = index, middle, and ring-pinky),  $D_{i,flx}$  and  $D_{i,ext}$  are the populational firing rate for the flexion and extension of the *i*th finger, respectively. The resultant  $R^2$  value and the root mean square error (RMSE) were used to quantify the performance of force estimation.

# 2) Force estimation using EMG amplitude

EMG channel selection and refinement. Even though the top 60 channels covered the most active areas when the corresponding fingers flexed or extended, there were substantial overlaps between fingers (Figure 3 B and C). Therefore, a refinement procedure was also performed to refine the EMG channel set for individual fingers using the multi-finger trials in the training set. Specifically, the EMG amplitude (RMS) was calculated using the average window for individual channels. For a given channel, a regression analysis was performed between the EMG amplitude and the smoothed forces of three fingers. Three R<sup>2</sup> values were obtained with each corresponding to one finger. If the R<sup>2</sup> value of the specific finger was larger than the remaining fingers, the given EMG channel was kept. Otherwise, it was removed from the EMG channel set. The procedure was repeated for all EMG channels before force estimation. The black curves in Figure 3 B and C encircled the channels used in the EMG-amp method for the flexion or extension of individual fingers.

Performance of force estimation. The multi-finger trials in the testing set were used to evaluate the force estimation performance of the EMG-amp method. The EMG amplitude was first calculated using the average window and then averaged across all retained EMG channels. Lastly, a bivariate linear regression analysis was performed between the smoothed

force data and the overall EMG amplitude of channel sets covering the flexors and extensors for individual fingers.

$$F_i = aA_{i,flx} + bA_{i,ext} \tag{2}$$

where  $F_i$  is the force of the *i*th finger (i = index, middle, and ring-pinky),  $A_{i,flx}$  and  $A_{i,ext}$  are the overall EMG amplitude for the flexion and extension of the *i*th finger, respectively.

 $\label{eq:table_interpolation} TABLE\ I$  Average MU number obtained from each trial

	Flexors		Extensors	
	Multi-finger	Single-finger	Multi-finger	Single-finger
Index	7.3±7.0	17.8±11.3	13.8±4.8	23.2±8.1
Middle	7.4±5.5	$15.7 \pm 13.0$	$15.0\pm2.4$	$21.8 \pm 6.0$
Ring- pinky	9.1±6.4	15.1±11.5	16.7±5.0	16.9±8.9

Mean ± Standard deviation

# III. RESULTS

Table I illustrates the average number of MUs decomposed from the multi-finger and the single-finger trials, respectively across all subjects before the refinement procedure. On average, more MUs can be obtained from the single-finger trial compared with the multi-finger trial, and more MUs can be obtained from the finger extensors compared with the finger flexors.

Figure 4 A illustrates the discharge event trains of MUs of the extensors and flexors of the middle finger from a representative multi-finger trial in the testing set. The thick blue and red curves represent the normalized populational firing rate of the extensors and flexors, respectively. The force estimation results using both the neural-drive and EMG-amp methods are shown in Figure 4 B. The estimated force using the neural-drive method can accurately track the actual force. From

approximately 8 to 13 second, there was an underestimation in the flexion force of the middle finger. From approximately 28 to 34 second, most of the MUs from both the flexors and extensors of the middle finger were active, and the overall firing rates of both increased. However, the estimated force within this period was small because the flexion firing rate and extension firing rate cancelled out in Equation (1). This co-contraction can lead to a smaller final force output. When the EMG-amp method was used, the overestimation and underestimation issue was more obvious, especially for the index finger.

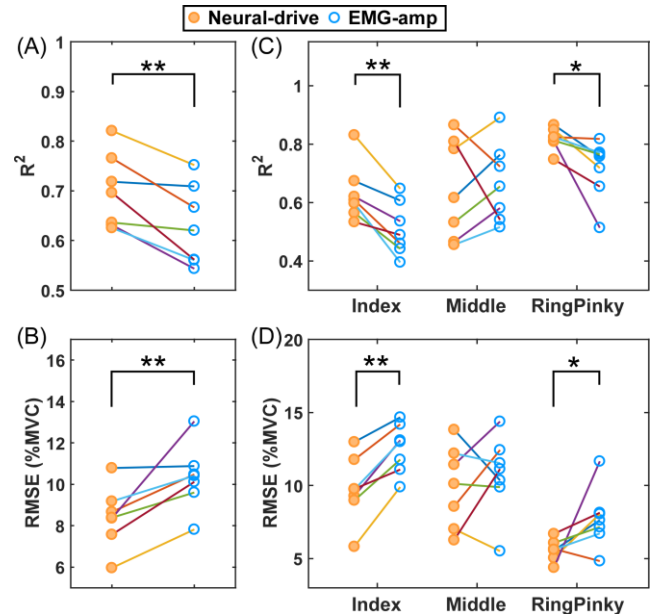


Fig. 5. The R<sup>2</sup> value (A) and the RMSE (B) across all trials of the neural-drive and EMG-amp methods. Symbols represent individual subjects. The R<sup>2</sup> value (C) and the RMSE (D) across all trials of the neural-drive and EMG-amp methods for individual fingers. \*, p<0.05. \*\*, p<0.01.

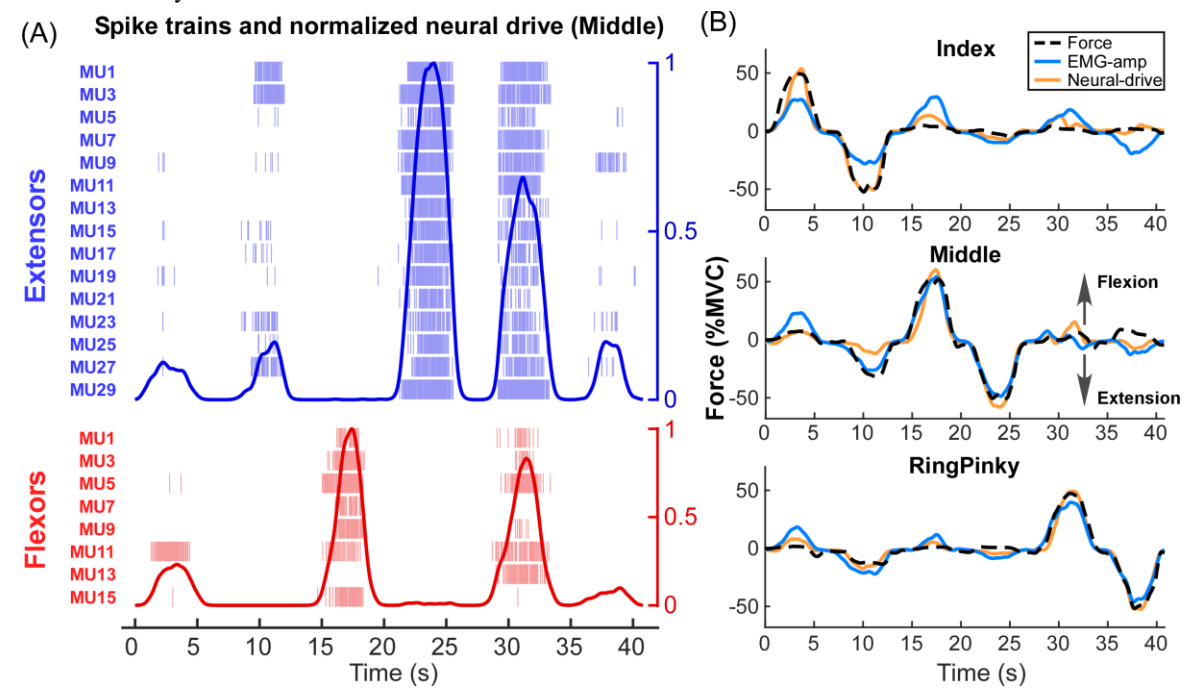


Figure 4: The discharge event trains and the normalized populational firing rate of MUs of the extensor and flexor of the middle finger from a representative multi-finger trial (A). Only odd-numbered MUs are shown for better illustration. The concurrent force estimation results of a single trial using both the neural-drive method and the EMG-amp method (B).

The R<sup>2</sup> value (Figure 5A) and the RMSE (Figure 5B) was first averaged across fingers and then across trials to represent the overall force estimation performance for individual subjects. Paired t-test showed that the R<sup>2</sup> value of the neural-drive method was significantly larger than that of the EMG-amp method (t(6)=4.06, p=0.0033, Cohen's d=1.5362), and the RMSE of the neural-drive method was significantly smaller than that of the EMG-amp method (t(6)=-3.55, p=0.0061, Cohen's d=-1.3408). In order to explore the force estimation performance for individual fingers, the two measurements were averaged across trials for individual fingers (Figure 5 C and D). Paired t-test revealed that the neural-drive method showed significantly better performance than the EMG-amp method for the index ( $R^2$ : t(6)=5.40, p=0.0008, Cohen's d= 2.0406; RMSE: t(6)=-7.08, p=0.0002, Cohen's d=-2.6755) and ring-pinky finger ( $R^2$ : t(6)=2.96, p=0.0126, Cohen's d=1.1195; RMSE: t(6)=-2.25, p=0.0325, Cohen's d=-0.8523). For the middle finger, there was no significant difference between the two methods ( $R^2$ : t(6)=-0.34, p=0.6266, RMSE: t(6)=-0.71, p=0.2517).

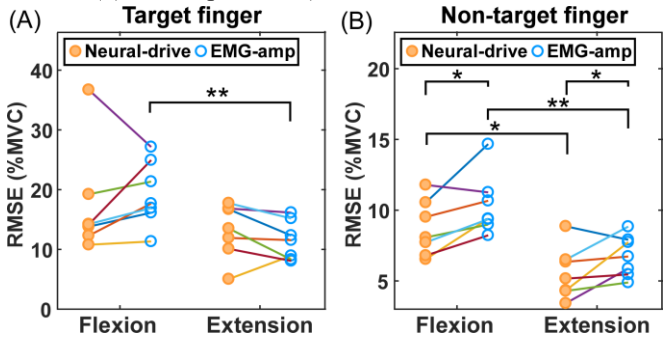


Fig. 6. The RMSE from the target finger during the flexion and extension of the target finger of both methods (A). The RMSE from the non-target finger during the flexion and extension of the target finger of both methods (B). Symbols represent individual subjects. \*, p<0.05. \*\*, p<0.01.

In order to further analyze the source of force estimation error, the RMSE was calculated within individual plateaus of the trapezoidal force target for individual fingers. Then, the average RMSE of the target finger was obtained separately for the flexion and extension conditions (Figure 6 A). Two-way (method: neural-drive vs. EMG-amp, and motion: flexion vs. extension) repeated measures ANOVA showed that only the motion type (F(1,6)=7.27, p=0.0358) had a significant influence on the RMSE with no interaction (p>0.05). Further post-hoc test with Holm–Bonferroni correction showed that the

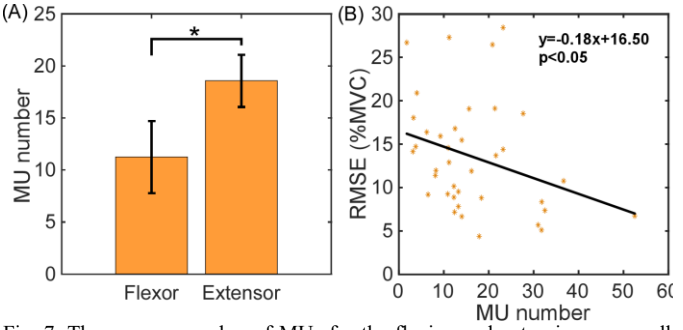


Fig. 7. The average number of MUs for the flexion and extension across all fingers (A). Correlation between the number of MUs and the RMSE (B). The error bars represent the standard deviation. \*, p<0.05.

RMSE during the flexion of the target finger was significantly larger than that during the extension of the target finger when the EMG-amp method was used (p<0.01, Cohen's d=1.3448). The average RMSE of the non-target finger was also calculated in a similar manner (Figure 6 B). The ANOVA showed that both the motion type (F(1,6)=20.70, p=0.0039) and the method (F(1,6)=18.53, p=0.0051) had a significant influence on the RMSE with no interaction (p>0.05). Further post-hoc test showed that the RMSE from the non-target finger of the neural-drive method was significantly smaller compared with that of the EMG-amp method, for both finger flexion (p<0.05, Cohen's d=-1.1166) and extension (p<0.05, Cohen's d=-0.7906). The RMSE during target-finger flexion was significantly larger than that during target-finger extension of the neural-drive (p<0.05, Cohen's d=1.2744) and the EMG-amp (p<0.01, Cohen's d=1.6755) method.

In addition, the number of MUs identified for the flexion or extension also varied significantly (Figure 7 A, t(6)= -3.4206, p=0.0141, Cohen's d=-1.2929). A correlation between the average RMSE and the number of MUs was performed for the flexion or extension of individual fingers (Figure 7 B). The results showed a weak but significant linear relation (R-value = -0.31) between the MU number and the RMSE (p<0.05), indicating that a larger number of MUs can lead to a smaller estimation error.

### IV. DISCUSSION

The objective of this study was to develop a neural decoding method to estimate flexion and extension forces of individual fingers concurrently using motoneuron discharge information. Our main results showed that the force estimation performance of the neural-drive method was significantly better (a higher correlation and a smaller error between the estimated force and the measured force), in comparison with that of the conventional EMG amplitude-based method, when the net forces of multiple fingers (especially the non-target fingers) need to be estimated concurrently. Our findings indicate that the continuous and concurrent decoding of individual finger force can potentially provide a robust human-machine interface that allows intuitive control of robotic hand with high dexterity.

In order to estimate both the flexion and extension forces of individual fingers, the MUs of the flexors and extensors were identified separately, and the neural drive signals to the flexors and extensors were then calculated separately. During finger flexion and extension, agonist-antagonist co-contraction can occur, and the final force output was determined by the force generated by both the flexors and the extensors. To address the agonist-antagonist co-contraction issue, a bivariate linear regression model was performed. The force estimation results for the middle finger in the representative trial (Figure 4) demonstrated that this model can reduce the influence of muscle co-contractions. For example, even when firing events were detected from both the flexors and extensors, the estimated force followed the measured total force accurately. However, in certain segments of the data, we also observed a large error between the estimated force and the measured force. This indicates that linear regression model might be insufficient

to fully capture the complex relation between the total force output and the neural drive signals of antagonists. In further studies, more complex models will be explored to address frequent muscle co-contractions, because co-contraction of antagonists is an important motor control strategy to improve joint stability [17, 18].

Besides agonist-antagonist co-contraction, finger enslaving can also lead to co-activation of multiple muscle compartments, controlling different fingers. To address the finger enslaving issue, the decomposed MU pools were further refined to only include MUs that associated with the finger force output. In contrast, a relatively larger force overestimation and underestimation was observed near peak flexion or extension forces when using the EMG-amp method, compared with the neural-drive method (Figure 4 B). The main source of error was that the channels selected for one finger can inevitably capture EMG activity of other fingers [26], even though a channel refinement procedure was performed. The neural-drive method alleviated these issues (Figure 5 and 6) because the MU pool refinement procedure removed MUs associated with the activation of other fingers. In addition, other factors might also lead to a better force estimation of the neural-drive method compared with the EMG-amp method, such as, the background noise and motion artifacts. It is because that the neural-drive method utilized the motoneuron discharge information, which was a binary time course. The background noise and motion artifacts could affect the extraction of several firing events, but have little influence on the calculation of the populational firing

Lastly, the results showed that more MUs can be identified from the extensors than the flexors (Figure 7 A), which is largely due to the fact that the FDS muscle is located far away from the skin surface compared with the EDC muscle. Therefore, action potentials from the EDC muscle may have a higher amplitude and a shorter duration compared with that of the FDS muscle, due to the spatial low-pass filtering effect of the tissue as a volume conductor [27]. The larger and shorter action potentials can help to isolate and identify more MUs from the EDC muscle. In addition, a previous simulation study has shown that the depth of the muscle can influence the number of identifiable MUs [28]. Our results further demonstrated that a better force estimation performance can be obtained if more MUs can be identified for force estimation, which provides a potential way to further improve the force estimation performance by increasing the number of MUs that can be identified through EMG decomposition.

In Figure 6, we compared the estimation errors for the target and non-target fingers, respectively, in order to investigate the source of the estimation errors of different methods. The 'target' finger only means that the subjects were instructed to adjust the force of that particular finger to follow the target force trajectory. The force of the non-target fingers was also measured and compared with the estimated force. When multiple fingers extend and flex dexterously, the force of all fingers need to be estimated accurately, which was the main goal of this study. Therefore, one advantage of the neural-drive method was an accurate force estimation of non-target fingers.

Namely, it can accurately estimate finger-specific force output.

It is true that the overall improvement based on RMSE of the neural-drive method seems to be small compared with the conventional EMG-amp method from Figure 5B, 5D and Figure 6. However, the RMSE was calculated as the average difference between the measured and estimated forces across the entire trial, which possibly reduced the large difference of estimation bias between two methods at some key timings, for example, during the flexion or extension peaks of the index finger in Figure 4B. In our previous study, it has been demonstrated that the neural-drive method can obtain a better force estimation performance compared with the conventional EMG amplitude-based method in the real-time condition, especially for prolonged muscle contractions when the EMG-amp method showed time-dependent increase in the estimation bias [14]. In the current study, in order to label the MUs for individual fingers, the MU separation vectors were obtained in advance. In the force estimation phase, the vectors were directly applied to the new EMG data to calculate the firing events, which makes our method readily applicable for the real-time condition. In our future study, we will investigate the estimation of dexterous finger force in real-time using the motoneuron discharge information. Compared with the conventional EMG-amp method, the neural-drive method is much more time consuming, which requires a more powerful hardware, and more investigation needs to be done to improve the efficiency of the algorithms. In addition, even though the accuracy of the firing event detection in the real-time condition can be assessed using the same measurement as the offline condition [14], the performance of the measurement decreases in the real-time condition, mainly because only a much shorter data segment (e.g. 1 second) is used compared with the offline condition.

The other limitation of the neural-drive method for real-time applications is that it cannot handle the situation of new MU recruitment after the initialization phase. It is likely that new MUs will be recruited during sustained muscle contraction. To identify those newly recruited MUs, the separation matrix needs to be updated periodically, potentially in a parallel background calculation. We also observed that the neural-drive method performed worse than the EMG-Amp method in some subjects as shown in Figures 5 and 6, partly due to a small number of MUs that can be extracted (Figure 7). Therefore, when the decomposition yield is low, the extracted MUs may not be able to accurately reflect the descending neural drive.

Only isometric muscle contractions were involved in this study. In future studies, dynamic contractions with joint movements will be investigated to see whether the neural-drive method can estimate the joint angle accurately when individual fingers flex and extend concurrently in a dexterous manner.

Lastly, even though the configuration contained 256 channels, the number of channels that was actually used during the analysis was much less (i.e., 60 channels or less). The 256 channels may be excessive/redundant for realistic applications. However, the electrode grid allows us to cover the entire muscle or muscle groups without knowing the optimal placement of the electrodes, and we can then select the best

channels based on the EMG signal properties as shown in Figure 3B. This built-in redundancy can accommodate non-functioning channels during the experiment by switching to a different channel. It can also accommodate electrode shift relative to targeted muscles during large movement by adjusting the set of channels based on EMG amplitude. We have discussed this in the revised manuscript.

## V. CONCLUSIONS

In this study, a reliable finger force estimation method was developed to estimate dexterous flexion and extension forces of individual fingers concurrently, based on the motoneuron discharge information of flexor and extensor muscles. Our results showed that the MU discharge information extracted from both finger flexors and extensors combined with a bivariate linear regression model can obtain a better force estimation performance compared with the conventional EMG amplitude-based method. Further development of this method can potentially provide a more robust human-machine interface based on surface EMG signals to achieve seamless and intuitive control of individual fingers of advanced robotic hands with high dexterity.

### REFERENCES

- [1] A. H. Al-Timemy, G. Bugmann, J. Escudero, and N. Outram, "Classification of finger movements for the dexterous hand prosthesis control with surface electromyography," *IEEE journal of biomedical and health informatics*, vol. 17, no. 3, pp. 608-618, 2013.
- [2] D. Tinoco Varela, F. Gudiño Peñaloza, and C. J. Villaseñor Rodelas, "Characterized Bioelectric Signals by Means of Neural Networks and Wavelets to Remotely Control a Human-Machine Interface," Sensors, vol. 19, no. 8, pp. 1923, 2019.
- [3] T. A. Kuiken, G. Li, B. A. Lock, R. D. Lipschutz, L. A. Miller, K. A. Stubblefield, and K. B. Englehart, "Targeted muscle reinnervation for real-time myoelectric control of multifunction artificial arms," *Jama*, vol. 301, no. 6, pp. 619-628, 2009.
- [4] M. A. Lebedev, and M. A. Nicolelis, "Brain-machine interfaces: past, present and future," *TRENDS in Neurosciences*, vol. 29, no. 9, pp. 536-546, 2006.
- [5] N. Nazmi, M. Abdul Rahman, S.-I. Yamamoto, S. Ahmad, H. Zamzuri, and S. Mazlan, "A review of classification techniques of EMG signals during isotonic and isometric contractions," *Sensors*, vol. 16, no. 8, pp. 1304, 2016.
- [6] A. Fougner, Ø. Stavdahl, P. J. Kyberd, Y. G. Losier, and P. A. Parker, "Control of upper limb prostheses: terminology and proportional myoelectric control—a review," *IEEE Transactions on neural systems and rehabilitation engineering*, vol. 20, no. 5, pp. 663-677, 2012.
- [7] A. A. Adewuyi, L. J. Hargrove, and T. A. Kuiken, "An analysis of intrinsic and extrinsic hand muscle EMG for improved pattern recognition control," *IEEE Transactions on Neural Systems and Rehabilitation Engineering*, vol. 24, no. 4, pp. 485-494, 2015.
- [8] J. Qi, G. Jiang, G. Li, Y. Sun, and B. Tao, "Intelligent human-computer interaction based on surface EMG gesture recognition," *IEEE Access*, vol. 7, pp. 61378-61387, 2019.
- [9] D. Farina, I. Vujaklija, M. Sartori, T. Kapelner, F. Negro, N. Jiang, K. Bergmeister, A. Andalib, J. Principe, and O. C. Aszmann, "Man/machine interface based on the discharge timings of spinal motor neurons after targeted muscle reinnervation," *Nature Biomedical Engineering*, vol. 1, no. 2, pp. 0025, 2017.
- [10] T. Kapelner, I. Vujaklija, N. Jiang, F. Negro, O. C. Aszmann, J. Principe, and D. Farina, "Predicting wrist kinematics from motor unit discharge timings for the control of active prostheses," *Journal of neuroengineering and rehabilitation*, vol. 16, no. 1, pp. 47, 2019.

- T. Kapelner, F. Negro, O. C. Aszmann, and D. Farina, "Decoding motor unit activity from forearm muscles: perspectives for myoelectric control," *IEEE Transactions on Neural Systems and Rehabilitation Engineering*, vol. 26, no. 1, pp. 244-251, 2018.
- [12] C. Dai, and X. Hu, "Finger Joint Angle Estimation Based on Motoneuron Discharge Activities," *IEEE J Biomed Health Inform*, vol. 24, no. 3, pp. 760-767, Mar, 2020.
- [13] M. D. Twardowski, S. H. Roy, Z. Li, P. Contessa, G. De Luca, and J. C. Kline, "Motor unit drive: a neural interface for real-time upper limb prosthetic control," *Journal of neural engineering*, vol. 16, no. 1, pp. 016012, 2018.
- [14] Y. Zheng, and X. Hu, "Real-time isometric finger extension force estimation based on motor unit discharge information," *J Neural Eng*, vol. 16, no. 6, pp. 066006, Oct 10, 2019.
- [15] C. Dai, Y. Cao, and X. Hu, "Prediction of individual finger forces based on decoded motoneuron activities," *Annals of biomedical engineering*, vol. 47, no. 6, pp. 1357-1368, 2019.
- [16] C. Dai, Y. Zheng, and X. Hu, "Estimation of muscle force based on neural drive in a hemispheric stroke survivor," *Frontiers in neurology*, vol. 9, pp. 187, 2018.
- [17] P. Aagaard, E. Simonsen, J. Andersen, S. Magnusson, F. Bojsen -Møller, and P. Dyhre - Poulsen, "Antagonist muscle coactivation during isokinetic knee extension," Scandinavian journal of medicine & science in sports, vol. 10, no. 2, pp. 58-67, 2000.
- [18] R. Baratta, M. Solomonow, B. Zhou, D. Letson, R. Chuinard, and R. D'ambrosia, "Muscular coactivation: the role of the antagonist musculature in maintaining knee stability," *The American journal of sports medicine*, vol. 16, no. 2, pp. 113-122, 1988.
- [19] V. M. Zatsiorsky, Z.-M. Li, and M. L. Latash, "Enslaving effects in multi-finger force production," *Experimental brain research*, vol. 131, no. 2, pp. 187-195, 2000.
- [20] Y. Zheng, and X. Hu, "Interference removal from electromyography based on independent component analysis,"

  IEEE Transactions on Neural Systems and Rehabilitation Engineering, vol. 27, no. 5, pp. 887-894, 2019.
- [21] C. Dai, and X. Hu, "Independent component analysis based algorithms for high-density electromyogram decomposition: Systematic evaluation through simulation," *Computers in Biology* and Medicine, vol. 109, pp. 171-181, 2019.
- [22] C. Dai, and X. Hu, "Independent component analysis based algorithms for high-density electromyogram decomposition: Experimental evaluation of upper extremity muscles," *Computers in Biology and Medicine*, vol. 108, pp. 42-48, 2019.
- [23] M. Chen, and P. Zhou, "A novel framework based on FastICA for high density surface EMG decomposition," *IEEE Transactions on Neural Systems and Rehabilitation Engineering*, vol. 24, no. 1, pp. 117-127, 2016.
- [24] D. Arthur, and S. Vassilvitskii, k-means++: The advantages of careful seeding, Stanford, 2006.
- [25] Y. Ning, X. Zhu, S. Zhu, and Y. Zhang, "Surface EMG decomposition based on K-means clustering and convolution kernel compensation," *IEEE J Biomed Health Inform*, vol. 19, no. 2, pp. 471-7, Mar, 2015.
- [26] X. Hu, N. L. Suresh, C. Xue, and W. Z. Rymer, "Extracting extensor digitorum communis activation patterns using high-density surface electromyography," *Frontiers in physiology*, vol. 6, pp. 279, 2015.
- [27] C. L. De, "Myoelectrical manifestations of localized muscular fatigue in humans," *Critical reviews in biomedical engineering*, vol. 11, no. 4, pp. 251-279, 1984.
- [28] D. Farina, F. Negro, M. Gazzoni, and R. M. Enoka, "Detecting the unique representation of motor-unit action potentials in the surface electromyogram," *Journal of neurophysiology*, vol. 100, no. 3, pp. 1223-1233, 2008.